

Model-Order Reduction of Moving Nonlinear Electromagnetic Devices

M. Nassar Albunni¹, Volker Rischmuller¹, Thomas Fritzsche¹, and Boris Lohmann²

¹Robert Bosch GmbH, Gerlingen 70839, Germany

²Institute of Automatic Control, Technical University of Munich, Garching D-85748, Germany

We present a new approach for generating fast simulation models of electromagnetic (EM) devices that contain moving components and magnetic materials with nonlinear properties. Our approach is based on generating low-dimensional simulation models that approximate the original spatially discretized models of electromagnetic field and their variations under conditions of component movement and material nonlinearity. The movement of the modeled device components is simulated by coupling the reduced-order EM field models weakly to the mechanical equations. We have successfully used our approach to generate a fast simulation model of a simple electromagnetic device with a moving component and nonlinear material properties.

Index Terms—BEM-FEM, electromagnetic devices, model-order reduction (MOR), proper orthogonal decomposition (POD), trajectory piecewise linear (TPWL) models, weakly coupled systems.

I. INTRODUCTION

ACCURATE simulation models that are able to analyze the behavior of real physical systems have become a base stone in the process of design and development of industrial devices. The permanently increasing complexity of modeled systems and the growing demand on improving models accuracy have been resulting in simulation models that have very large dimensionality. However, the requirements to simulate such models may rapidly go beyond the available time and computational resources.

Model-order reduction techniques present a solution for the complexity-accuracy dilemma. This is due to their ability to generate compact simulation models—having low number of equations—starting from the original high-complexity ones. The accuracy of the generated models can be guaranteed in some segments of the frequency domain or around several trajectories in the time domain.

Electromagnetism is one of the fields where model-order reduction techniques have been receiving a growing interest. Their ability to generate compact simulation models of electromagnetic (EM) devices starting from their spatially discretized linear models has been demonstrated in several works [5], [20]–[22]. Less focus has been put on applying model-order reduction techniques to the *nonlinear* models of electromagnetic devices. A major contribution in this field is the work in [15] in which the authors applied the trajectory piecewise linear (TPWL) models approach [17] to generate a compact approximation model of a magnetic device with nonlinear materials properties. However, a crucial issue that has not been addressed in most of the previous works is considering the movement of the modeled device components in the generation of the reduced-order models. This can be traced back to the significant changes that can occur in the electromagnetic field model upon the movement of one or more of the modeled device components.

In this work, we propose a new approach that tackles the challenge of including the effects of both components movement

and materials nonlinearity in the reduced-order models of electromagnetic devices. The approach exploits model-order reduction techniques to approximate the large scale nonlinear models of the electromagnetic field by reduced-order ones having a much lower number of equations. The reduced-order EM field models are weakly coupled to the mechanical equations in order to handle the movement of the device components. The position information that are obtained from solving the mechanical equations are used to update the position-dependent terms in the reduced-order EM field models according to the new components positions.

The remainder of this paper is organized as follows. In Section II, a short introduction to order reduction approaches of nonlinear dynamic systems is presented, with a special focus on the TPWL models approach and the proper orthogonal decomposition (POD). In Section III, an overview on the time domain analysis of electromagnetic devices including motion is presented, providing more information on the coupled boundary element-finite element modeling (BEM-FEM) approach. The new approach for generating fast simulation models of moving nonlinear electromagnetic devices is presented in Section IV. Whereas in Section V, the results of applying the proposed approach to generate a compact model of a moving electromagnetic device with nonlinear materials properties are illustrated. Finally, a conclusion is drawn in Section VI.

II. ORDER REDUCTION OF NONLINEAR DYNAMIC SYSTEMS

The common aim of all model-order reduction approaches is to generate low-order approximation models of dynamic systems starting from their original high-order models. The order of a system in this context refers to the number of variables that are contained in the state vector of the system model. In the past two decades, several approaches for generating reduced-order models of large scale nonlinear dynamic systems have been proposed. Their development has been aiming at reducing the complexity of the generated reduced-order models, extending their validity range, and shortening their extraction time. Unfortunately, the inherited complexity of nonlinear systems has made it difficult to find an approach that fulfills all the above mentioned aims at once. Hence, the proposed approaches have achieved different compromises between the three conflicting

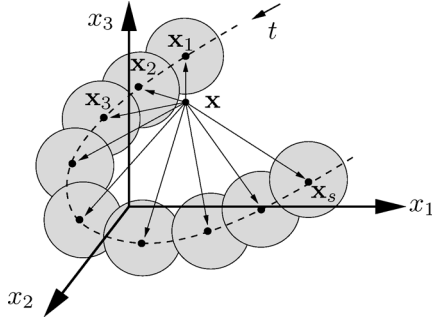


Fig. 1. Approximating a nonlinear dynamic system by a weighted sum of linearized models along some simulation trajectory $\mathbf{x}(t)$. Each of the shaded areas symbolically represents the validity region of a certain linearized model in the state space of the underlying system. Those regions are in general dissimilar in their shapes and sizes.

aims. A comprehensive survey in this field can be found in [13] and [14]. A recent approach that has been receiving a growing interest is the TPWL models [17]. This is due to its ability to generate low-order approximation models of dynamic systems with strong nonlinear behavior, while keeping the complexity of building and simulating the reduced models within acceptable bounds.

A. TPWL Models

Given a nonlinear dynamic system of order n :

$$\frac{d}{dt}\mathbf{g}(\mathbf{x}(t)) = \mathbf{f}(\mathbf{x}(t)) + \mathbf{B}\mathbf{u}(t) \quad \mathbf{x} \in \mathbb{R}^n. \quad (1)$$

A reduced-order model of order $k \ll n$ can be generated using the TPWL models approach [17] as follows. (For the sake of clarity, the explicit notation of time dependency in $\mathbf{x}(t)$, $\mathbf{u}(t)$ is dropped.)

- 1) Simulate the nonlinear system (1) with one or more typical excitation signals \mathbf{u} .
- 2) Linearize the nonlinear terms in (1) at s different points $\{\mathbf{x}_1, \mathbf{x}_2, \dots, \mathbf{x}_s\}$ along the simulated trajectories \mathbf{x} , in such a way that the nonlinear functions $\mathbf{g}(\mathbf{x})$ and $\mathbf{f}(\mathbf{x})$ can be locally approximated in the neighborhood of each of the linearization point \mathbf{x}_i by

$$\begin{cases} \mathbf{g}(\mathbf{x}) \approx \mathbf{g}(\mathbf{x}_i) + \mathbf{G}_i(\mathbf{x} - \mathbf{x}_i) \\ \mathbf{f}(\mathbf{x}) \approx \mathbf{f}(\mathbf{x}_i) + \mathbf{W}_i(\mathbf{x} - \mathbf{x}_i) \end{cases} \quad (2)$$

where \mathbf{G}_i , \mathbf{W}_i are respectively the Jacobian matrices of the nonlinear functions $\mathbf{g}(\mathbf{x})$ and $\mathbf{f}(\mathbf{x})$ at the linearization point \mathbf{x}_i (Fig. 1).

- 3) Define a distance based weighting function $\alpha(\mathbf{x})$ and approximate the nonlinear system (1) by a weighted sum of the linearized models:

$$\begin{aligned} \frac{d}{dt} \sum_{i=1}^s \alpha_i(\mathbf{x}) [\mathbf{g}(\mathbf{x}_i) + \mathbf{G}_i(\mathbf{x} - \mathbf{x}_i)] \\ = \sum_{i=1}^s \alpha_i(\mathbf{x}) [\mathbf{f}(\mathbf{x}_i) + \mathbf{W}_i(\mathbf{x} - \mathbf{x}_i)] + \mathbf{B}\mathbf{u}. \end{aligned} \quad (3)$$

The weighting coefficients $(\alpha_1, \dots, \alpha_s)$ determine the contribution of each of the linearized models (2) to the

overall model (3). Their values at each simulation step are calculated as a function α of the distances between the current solution point \mathbf{x} and all the linearization points $\{\mathbf{x}_1, \mathbf{x}_2, \dots, \mathbf{x}_s\}$, in such a way that the value of a weighting coefficient α_i increases when the state variables vector \mathbf{x} approaches the linearization point \mathbf{x}_i

$$\begin{cases} (\alpha_1, \dots, \alpha_s) = \alpha(\mathbf{x}, \{\mathbf{x}_1, \dots, \mathbf{x}_s\}) \\ \sum_{i=1}^s \alpha_i = 1. \end{cases} \quad (4)$$

- 4) Use model-order reduction techniques to find a low-order approximation of the ensemble of linearized models (3). This can be performed by exploiting any of the techniques of order reduction of linear dynamic systems. However, in this work we use the proper orthogonal decomposition POD to perform this task. The reduction using POD corresponds to finding a global projection matrix \mathbf{V} that has the ability to approximate the state variables vector $\mathbf{x} \in \mathbb{R}^n$ optimally in the subspace spanned by its columns as it will be shown in the next paragraph.
- 5) Reduce the order of all the linearized models in (3) from order n to order k , where $k \ll n$ is the number of columns contained in \mathbf{V} . The reduction is done by projecting the ensemble of linearized models onto the subspace spanned by the columns of the projection matrix \mathbf{V} :

$$\frac{d}{dt} \sum_{i=1}^s \alpha_i(\mathbf{z}) [\mathbf{G}_{r,i}\mathbf{z} + \mathbf{g}_{r,i}] = \sum_{i=1}^s \alpha_i(\mathbf{z}) [\mathbf{W}_{r,i}\mathbf{z} + \mathbf{f}_{r,i}] + \mathbf{B}_r\mathbf{u} \quad (5)$$

where

$$\begin{aligned} \mathbf{z} &\in \mathbb{R}^k \\ \mathbf{x} &= \mathbf{V}\mathbf{z} \\ \mathbf{g}_{r,i} &= \mathbf{V}^T(\mathbf{g}(\mathbf{x}_i) - \mathbf{G}_i\mathbf{x}_i) \\ \mathbf{f}_{r,i} &= \mathbf{V}^T(\mathbf{f}(\mathbf{x}_i) - \mathbf{W}_i\mathbf{x}_i) \\ \mathbf{G}_{r,i} &= \mathbf{V}^T\mathbf{G}_i\mathbf{V}, \mathbf{W}_{r,i} = \mathbf{V}^T\mathbf{W}_i\mathbf{V}, \mathbf{B}_r = \mathbf{V}^T\mathbf{B}. \end{aligned}$$

To summarize, the TPWL models approach approximates the nonlinear model in (1) by a weighted sum of linearized models (3). Then the number of equations in all linearized models is reduced to generate the final compact low-order model (5).

B. Proper Orthogonal Decomposition POD

The proper orthogonal decomposition is a method for building a low-order approximation of both linear and nonlinear dynamic systems. It is based on formulating the behavior of dynamic systems as a function of a low number of orthogonal vectors that are extracted from the partial observations of the system variables [2].

If a number of p observations of the n variables of a dynamic system are assembled in a so-called snapshots matrix:

$$\mathbf{X} = [\mathbf{x}_1, \dots, \mathbf{x}_p] \quad \mathbf{X} \in \mathbb{R}^{n \times p}$$

the POD approximates the high-dimensional observations in \mathbf{X} as linear combination of a low number of orthogonal vectors

$$\hat{\mathbf{X}} = \mathbf{V}\mathbf{X}_r \quad \text{such that} \quad \hat{\mathbf{X}} \approx \mathbf{X}$$

where

$$\left. \begin{aligned} \mathbf{V} &= [\mathbf{v}_1, \dots, \mathbf{v}_k] & \mathbf{V} &\in \mathbb{R}^{n \times k} \\ \mathbf{X}_r &= [\mathbf{x}_{r1}, \dots, \mathbf{x}_{rp}] & \mathbf{X}_r &\in \mathbb{R}^{k \times p} \end{aligned} \right\} k < \text{rank}(\mathbf{X}).$$

There are several popular approaches to construct the orthogonal vectors of the matrix \mathbf{V} based on the information contained in the snapshots matrix, such as the principal components analysis PCA, the Karhunen–Loeve decomposition KLD, and the singular values decomposition SVD. However, the authors in [12] have proved the equivalence of the three methods. In the SVD-based approach, the optimal approximation of \mathbf{X} is formulated as a matrix approximation problem. The approximation accuracy can be expressed in minimizing a certain norm of the error matrix

$$\mathbf{E} = \mathbf{X} - \mathbf{V}\mathbf{X}_r.$$

This minimization problem can be exactly solved by finding the singular values decomposition $\mathbf{X} = \mathbf{U}\mathbf{\Sigma}\mathbf{W}^T$ and taking the optimal basis vectors as the columns of \mathbf{U} and the reduced-order snapshots matrix as $\mathbf{X}_r = \mathbf{\Sigma}\mathbf{W}^T$. However, in order to get a low rank approximation of \mathbf{X} , only the first k columns of \mathbf{U} are taken in the matrix \mathbf{V} . This, in turn, guarantees minimizing both the 2-induced and the Frobenius norms of the error matrix:

$$\min \|\mathbf{E}\|_F = \min \|\mathbf{X} - \mathbf{V}\mathbf{X}_r\|_F = \left(\sum_{i=k+1}^{\text{rank } \mathbf{X}} \sigma_i^2(\mathbf{X}) \right)^{1/2}$$

assuming that $\sigma_k > \sigma_{k+1}$. (6)

It can be clearly seen in (6) that the approximation optimality can be improved by taking more columns of \mathbf{U} in the matrix \mathbf{V} . Therefore, a tradeoff between the required approximation accuracy and the dimensionality of the reduced-order approximation has to be found. This tradeoff can be determined by giving the required level of accuracy [e.g., maximum allowed error norm in (6)] and finding the required number of basis vectors to achieve it.

It is worth mentioning that in the case where the number of snapshots is smaller than the dimensions of the observed systems, the optimal basis vectors can be found in a cheaper way by performing an eigenvalues decomposition of the autocorrelation matrix $\mathbf{\Psi} = \mathbf{X}^T\mathbf{X}$, and using the resulting eigenvectors to construct the optimal basis vectors of \mathbf{V} as shown in [1].

It should be stressed that the optimality of the POD approximation is only guaranteed for the vectors that are contained in the snapshots matrix \mathbf{X} . Therefore, in order to get a good approximation of the behavior of a dynamic system in certain segments of its state space, the system has to be simulated using suitable excitation signals $\mathbf{u}(t)$ in order to generate enough observations $[\mathbf{x}_1, \dots, \mathbf{x}_p]$ that represent the dominant behavior of the dynamic system in the considered segments of the state space.

III. TIME DOMAIN ANALYSIS OF ELECTROMAGNETIC DEVICES INCLUDING MOTION

A. General Overview

The dynamic analysis of electromechanical systems including motion requires the solution of the coupled electromagnetic-mechanical equations. However in a large class of

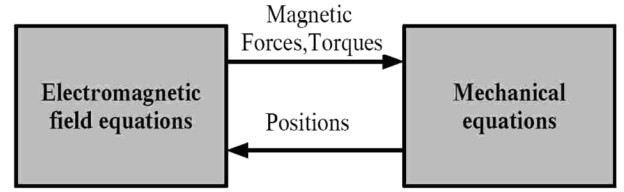


Fig. 2. Weak electromechanical coupling approach.

industrial applications, the state variables of the mechanical equations are much slower than the ones of the electromagnetic field equations. Thus, if the simulation time step is chosen to be small enough, then the two systems of equations can be solved alternately in the so called “weak electromechanical coupling” approach [9] as it is shown in Fig. 2:

The main steps of the weak coupling scheme can be summarized as follows:

- 1) *Solving the electromagnetic field equations:* In low-frequency limits, the spatial discretization of the transient formulations of electromagnetic field using one of the finite discretization methods [e.g., the finite element (FE), finite difference (FD), or the coupled finite-element boundary-element methods (BEM-FEM)] commonly produces large-order nonlinear systems of ordinary differential equations or differential algebraic equations [6]. By applying a certain time integration scheme, the values of the EM field variables can be found and the corresponding magnetic forces and torques can be calculated.
- 2) *Solving the mechanical equations:* Based on the calculated values of magnetic forces and torques, the mechanical equations can be solved in order to update the device components positions. If movement of rigid bodies is considered, the movement of an object can be described as a translation of its center of gravity with respect to a reference coordinate frame, and a rotation of its own coordinate frame with respect to the reference frame. Therefore, a maximum number of six equations per moving object are required for describing its movement in 3-D space.
- 3) *Updating the electromagnetic field equations according to the new components positions:* When one or more of the device components move, the electromagnetic field model has to be updated. Several strategies can be exploited to perform this update. In the remeshing approach [11], a new discretization mesh with a possibly new number of nodes has to be generated whenever the device components change their positions. Whereas in the sliding mesh approach [4], which is particularly popular for handling rotational movement, the unknown variables that are located on the interfaces between the sliding meshes are permuted upon components rotation. Finally, in the coupled boundary elements finite elements method BEM-FEM, a group of boundary matrices has to be recalculated whenever a device component changes its position.

After updating the electromagnetic field equations, a new simulation cycle can be started according to the aforementioned steps. However, for complex EM devices, solving the high-dimensional nonlinear EM field equations can be very time and computer resources consuming. Therefore, a significant speed

up in the simulation time can be achieved by approximating the original systems of equations by compact ones having much lower number of equations.

Motivated by this fact, this research work exploits model-order reduction techniques to build low-order approximation models of EM field starting from their original high-dimensional spatially discretized ones. The coupled BEM-FEM is chosen to generate the full order models of EM field due to its advantages in keeping both the number and the ordering of the EM field variables constant during components movement, as it is shown in detail in the next paragraph.

B. Time Domain Analysis Using the Coupled BEM-FEM

The modeling scheme reviewed here starts from the potential based magneto(quasi)static formulation of Maxwell equations:

$$\text{rot } \nu \text{ rot } \vec{A} = \vec{j}_E + \vec{j}_S \quad (7)$$

$$\text{div}(\vec{j}_E + \vec{j}_S) = 0 \quad (8)$$

$$\vec{j}_E = -\sigma \partial_t (\vec{A} + \text{grad} \Phi) \quad (9)$$

where

\vec{A}	magnetic vector potential;
ν	relative reluctivity $\nu = \nu(\vec{A})$;
\vec{j}_E	eddy current density;
\vec{j}_S	impressed source current density;
σ	electrical conductivity;
Φ	electric scalar potential.

The relative reluctivity ν is dependent in general on the vector \vec{A} of EM field variables [8], this dependency in turn makes (7) nonlinear.

When applying the BEM-FEM method to discretize the (7)–(9) in 3-D space, the conducting and the magnetic parts of the devices are discretized using finite elements, whereas the boundary elements are used to cover the surrounding surfaces. The spatial discretization can be carried out using a nodal-based approach [10], [19] or an edge-elements-based one [16]. The latter approach is based on treating the variables of the EM field as differential forms [3], a treatment that has been proved to produce in general the right solution of Maxwell problems [7]. However, the detailed comparison between the two approaches is out of the scope of this work. The important fact concerning the presented work is that both of the discretization approaches in [10], [16], [19] produce a system of differential algebraic equations DAE of the form:

$$\begin{cases} \mathbf{C}\dot{\mathbf{a}} + \mathbf{K}(\mathbf{a})\mathbf{a} - \mathbf{T}\mathbf{q} = \mathbf{r}_s \\ \mathbf{H}(\mathbf{x})\mathbf{a} + \mathbf{G}(\mathbf{x})\mathbf{q} = \mathbf{r}_{s\Gamma} \end{cases} \quad (10)$$

where

\mathbf{a}	degrees of freedom of magnetic vector potential;
\mathbf{q}	Neumann data of the exterior boundary problem;
\mathbf{C}	damping matrix;

$\mathbf{K}(\mathbf{a})$	field-dependent stiffness matrix;
\mathbf{T}	constant boundary matrix;
\mathbf{H}, \mathbf{G}	position-dependent boundary matrices;
\mathbf{r}_s	contribution of the impressed current density;
$\mathbf{r}_{s\Gamma}$	contribution of the external sources of magnetic vector potential.

By eliminating the algebraic variables \mathbf{q} from (10) and assuming—without the loss of generality—that all sources of magnetic vector potential are modeled in \mathbf{r}_s (i.e. $\mathbf{r}_{s\Gamma} = 0$), then the EM field model can be written as

$$\mathbf{C}\dot{\mathbf{a}} + [\mathbf{K}(\mathbf{a}) + \mathbf{K}^{\text{BEM}}(\mathbf{x})]\mathbf{a} = \mathbf{r}_s \quad (11)$$

where

$$\mathbf{K}^{\text{BEM}}(\mathbf{x}) = \mathbf{T}\mathbf{G}^{-1}(\mathbf{x})\mathbf{H}(\mathbf{x}). \quad (12)$$

The dependency of the matrix $\mathbf{K}^{\text{BEM}}(\mathbf{x})$ on the position \mathbf{x} originates from the dependency of the boundary matrices \mathbf{G}, \mathbf{H} on the positions of the modeled device components.

The vector \mathbf{r}_s contains in general the contributions of the impressed current densities. However, in this work we consider the case where the sources of excitation are current driven coils with homogenous current densities throughout their cross sections [18]. Under this assumption, the vector \mathbf{r}_s can be written as

$$\mathbf{r}_s = \sum_{k=1}^m \mathbf{c}_s^{(k)} i^{(k)} \quad (13)$$

where $\mathbf{c}_s^{(1)}, \dots, \mathbf{c}_s^{(m)}$ are vectors containing the coefficients of the excitation coils $1, \dots, m$, and $i^{(1)}, \dots, i^{(m)}$ are their respective impressed currents.

In order to model components movement, the induced electromagnetic forces and torques in those components have to be calculated, and the equations that describe both their rotational and translational movement have to be solved. A popular method to calculate electromagnetic forces is to integrate the Maxwell stress tensor [9], [10] over the boundary s_k of an object k giving the total electromagnetic force $\vec{f}_{\text{mag},k}$ that is acting on it:

$$\vec{f}_{\text{mag},k} = \int_{s_k} (\vec{f}_n + \vec{f}_t) ds \quad (14)$$

$$\vec{f}_n = \frac{1}{2} \left(\frac{B_n^2}{\mu_0} - \mu_0 H_t^2 \right) \vec{n}, \quad \vec{f}_t = B_n \vec{H}_t \quad (15)$$

where

\vec{B}	magnetic induction;
\vec{H}	magnetic field strength;
\vec{n}	unit vector in the normal direction;
μ_0	magnetic permeability in vacuum.

The tangential vector \vec{H}_t and the normal induction B_n can be calculated from the solution vectors of discretized model (10). The spatially discretized form of (14), (15) can be formulated as

$$\mathbf{f}_{\text{mag},k} = [\mathbf{a} \quad \mathbf{q}] \underbrace{\begin{bmatrix} \tilde{\mathbf{R}}_{11}^{(k)} & \tilde{\mathbf{R}}_{12}^{(k)} \\ \tilde{\mathbf{R}}_{21}^{(k)} & \tilde{\mathbf{R}}_{22}^{(k)} \end{bmatrix}}_{\tilde{\mathbf{R}}^{(k)}} [\mathbf{a} \quad \mathbf{q}] \quad (16)$$

where the index k denotes the k^{th} object for which the EM force is calculated. The matrices $\tilde{\mathbf{R}}^{(k)}$ are constant and do not need to be updated upon components movement. However, when eliminating the variables \mathbf{q} from (16) the resulting matrices $\mathbf{R}^{(k)}$ become position dependent, due to the use of the position-dependent matrices \mathbf{G}, \mathbf{H} (10) in the elimination step:

$$\mathbf{f}_{\text{mag},k} = \mathbf{a}^T \mathbf{R}^{(k)}(\mathbf{x}) \mathbf{a}. \quad (17)$$

The magnetic torques can be derived in a very similar way, and the rotational movement of the device components can be handled by solving Euler's equations.

Due to the limited editorial space, we will restrict ourselves in this work to the case of a translational movement of a single object, additionally we assume that the source of EM field is a single current driven coil (13). However, the extension to the case of rotational movement, multi moving objects, and multi excitation coils is straightforward. Consequently, the overall model considered in this work consists of the high-order nonlinear EM field model:

$$\begin{cases} \mathbf{C}\dot{\mathbf{a}} + [\mathbf{K}(\mathbf{a}) + \mathbf{K}^{\text{BEM}}(\mathbf{x})] \mathbf{a} = \mathbf{c}_s i \\ \mathbf{f}_{\text{mag}} = \mathbf{a}^T \mathbf{R}(\mathbf{x}) \mathbf{a} \end{cases} \quad (18)$$

weakly coupled to the low-order mechanical model:

$$\mathbf{M}\ddot{\mathbf{x}} + \mathbf{D}\dot{\mathbf{x}} + \mathbf{K}_m \mathbf{x} = \mathbf{f}_{\text{mag}} \quad (19)$$

where $\mathbf{M}, \mathbf{D}, \mathbf{K}_m$ are respectively the mass, damping, and the stiffness matrices of the mechanical equations, and \mathbf{x} is the position vector of the device components.

IV. A SCHEME FOR MODEL-ORDER REDUCTION OF MOVING NONLINEAR ELECTROMAGNETIC DEVICES

The structure of the weakly coupled models (18), (19) represents a challenge for applying order reduction techniques due to the following difficulties.

- The nonlinearity of the electromagnetic field model which appears in the term $\mathbf{K}(\mathbf{a})\mathbf{a}$.
- The explicit dependency of the electromagnetic field model (18) on the position variables \mathbf{x} of the weakly coupled mechanical equations (19), which appears in the position-dependent terms $\mathbf{K}^{\text{BEM}}(\mathbf{x})$ and $\mathbf{R}(\mathbf{x})$.

The nonlinearity of the EM field model can be tackled by applying the TPWL models approach to approximate the nonlinear term $\mathbf{K}(\mathbf{a})\mathbf{a}$ by a weighted sum of its linearized functions at several linearization points \mathbf{a}_i . However, the problem of the explicit dependency of the EM field model (18) on the position variables of the weakly coupled mechanical equations remains unsolved even after applying the TPWL model. In order to overcome this

challenge, we propose to use the position information $\mathbf{x}(t)$ that are obtained from solving the mechanical equations (19) to approximate the position-dependent terms $\mathbf{K}^{\text{BEM}}(\mathbf{x}), \mathbf{R}(\mathbf{x})$ in the EM field equations (18) at each simulation step. The approximation can be realized by interpolating a group of their values $\mathbf{K}_j^{\text{BEM}}(\mathbf{x}), \mathbf{R}_j(\mathbf{x})$ at several position points \mathbf{x}_j along the movement path.

The proposed scheme for generating reduced-order EM devices models is detailed in the following.

- 1) Simulate the high-order nonlinear EM field model (18) weakly coupled to the mechanical model (19) with one or more typical excitation signals $i(t)$.
- 2) Linearize the nonlinear term $\mathbf{K}(\mathbf{a})\mathbf{a}$ at s_1 different points $\{\mathbf{a}_1, \dots, \mathbf{a}_{s_1}\}$ along the simulated trajectories $\mathbf{a}(t)$.

$$\begin{aligned} \mathbf{K}(\mathbf{a})\mathbf{a} &\approx \mathbf{K}(\mathbf{a}_i)\mathbf{a}_i + \left. \frac{d}{d\mathbf{a}} [\mathbf{K}(\mathbf{a})\mathbf{a}] \right|_{\mathbf{a}_i} (\mathbf{a} - \mathbf{a}_i) \\ &\approx \mathbf{g}_i + \mathbf{L}_i \mathbf{a} \end{aligned} \quad (20)$$

where

$$\mathbf{L}_i = \left. \frac{d}{d\mathbf{a}} [\mathbf{K}(\mathbf{a})\mathbf{a}] \right|_{\mathbf{a}_i}, \quad \mathbf{g}_i = \mathbf{K}(\mathbf{a}_i)\mathbf{a}_i - \mathbf{L}_i \mathbf{a}_i.$$

- 3) Extract the values of the position-dependent matrices $\mathbf{K}^{\text{BEM}}(\mathbf{x}), \mathbf{R}(\mathbf{x})$ at s_2 different positions $\{\mathbf{x}_1, \dots, \mathbf{x}_{s_2}\}$ along the movement path $\mathbf{x}(t)$.
- 4) Build an approximation for the electromagnetic field model (18) by approximating the nonlinear term $[\mathbf{K}(\mathbf{a})\mathbf{a}]$ by a weighted sum of its linearized functions (20), and approximating the position-dependent terms by interpolating their s_2 extracted values:

$$\mathbf{C}\dot{\mathbf{a}} + \sum_{i=1}^{s_1} \alpha_i(\mathbf{a})[\mathbf{g}_i + \mathbf{L}_i \mathbf{a}] + \sum_{j=1}^{s_2} \beta_j(\mathbf{x}) \mathbf{K}_j^{\text{BEM}} \mathbf{a} = \mathbf{c}_s i \quad (21)$$

$$\mathbf{f}_{\text{mag}} = \mathbf{a}^T \left[\sum_{j=1}^{s_2} \beta_j(\mathbf{x}) \mathbf{R}_j \right] \mathbf{a} \quad (22)$$

$$(\alpha_1, \dots, \alpha_{s_1}) = \boldsymbol{\alpha}(\mathbf{a}, \{\mathbf{a}_1, \dots, \mathbf{a}_{s_1}\}) \quad (23)$$

$$(\beta_1, \dots, \beta_{s_2}) = \boldsymbol{\beta}(\mathbf{x}, \{\mathbf{x}_1, \dots, \mathbf{x}_{s_2}\})$$

$$\sum_{i=1}^{s_1} \alpha_i = 1 \quad \sum_{j=1}^{s_2} \beta_j = 1. \quad (24)$$

The weighting function $\boldsymbol{\alpha}$ should be constructed in such a way that a linearized function (20) gets a higher weighting value α_i when the variables vector \mathbf{a} of EM field approaches the linearization point \mathbf{a}_i . Similarly, the weighting function $\boldsymbol{\beta}$ should give higher weighting values β_j for the position-dependent matrices $\mathbf{K}_j^{\text{BEM}}, \mathbf{R}_j$ when the position vector $\mathbf{x}(t)$ approaches the position point \mathbf{x}_j .

- 5) Assemble a group of p solution vectors of the high-order nonlinear EM field equations (18) in a so called snapshots matrix $[\mathbf{a}_1, \mathbf{a}_2, \dots, \mathbf{a}_p] \in \mathbb{R}^{n \times p}$, and apply the POD to generate a projection matrix $\mathbf{V} \in \mathbb{R}^{n \times k}$ that realizes an optimal approximation (6) of the ensemble of the solutions that are contained in the snapshots matrix.

- 6) Reduce the order of the model (21), (22) by projecting all the extracted models onto the subspace spanned by the columns of the projection matrix \mathbf{V}

$$\mathbf{C}_r \dot{\mathbf{a}}_r + \sum_{i=1}^{s_1} \alpha_i(\mathbf{a}_r) [\mathbf{g}_{ri} + \mathbf{L}_{ri} \mathbf{a}_r] \text{fill} + \sum_{j=1}^{s_2} \beta_j(\mathbf{x}) \mathbf{K}_{rj}^{\text{BEM}} \mathbf{a}_r = \mathbf{c}_{sr} \dot{t} \quad (25)$$

$$\mathbf{f}_{\text{mag}} = \mathbf{a}_r^T \left[\sum_{j=1}^{s_2} \beta_j(\mathbf{x}) \mathbf{R}_{rj} \right] \mathbf{a}_r \quad (26)$$

where $\mathbf{a} = \mathbf{V} \mathbf{a}_r$, $\mathbf{a} \in \mathbb{R}^n$, $\mathbf{a}_r \in \mathbb{R}^k$, and $k \ll n$

$$\begin{aligned} \mathbf{C}_r &= \mathbf{V}^T \mathbf{C} \mathbf{V} & \mathbf{L}_{ri} &= \mathbf{V}^T \mathbf{L}_i \mathbf{V} \\ \mathbf{R}_{ri} &= \mathbf{V}^T \mathbf{R}_i \mathbf{V} & \mathbf{K}_{ri}^{\text{BEM}} &= \mathbf{V}^T \mathbf{K}_i^{\text{BEM}} \mathbf{V} \\ \mathbf{g}_{ri} &= \mathbf{V}^T \mathbf{g}_i & \mathbf{c}_{sr} &= \mathbf{V}^T \mathbf{c}_s \end{aligned}$$

and the weighting function (23) becomes dependent on the distance in the reduced-order subspace

$$(\alpha_1, \dots, \alpha_{s_1}) = \boldsymbol{\alpha}(\mathbf{a}_r, \{\mathbf{a}_{r1}, \dots, \mathbf{a}_{rs_1}\}). \quad (27)$$

The final reduced-order model of the electromagnetic field (25), (26) is of order k (i.e. having k unknowns in the variables vector \mathbf{a}_r) which is much lower than the order n of the original model (18). Therefore, it offers a significant reduction in the required simulation time and computational resources.

The decoupled approximation of the position-dependent terms and the EM field variables dependent terms in the electromagnetic field model (25), (26) allows the user to control the approximation accuracy of both terms independently. This can be done by controlling the parameters s_1 and s_2 respectively. Moreover, the decoupled approximation of the position-dependent terms allows to couple the reduced-order EM field model (25), (26) to any parametric mechanical model in order to simulate the components movement. This in turns makes the overall coupled electromagnetic-mechanical models parametric and enables exploiting them in the design optimization and robustness analysis of electromechanical systems.

The simulation cycle of the overall reduced-order device model can be performed according to the following algorithm:

Algorithm 1 Simulating the reduced-order models of electromagnetic devices

- 1: define initial conditions $\mathbf{a}_r^0 = \mathbf{V}^T \mathbf{a}^0$, \mathbf{x}^0 , $\dot{\mathbf{x}}^0$
- 2: define a simulation time vector $[t^1, t^2, \dots, t^N]$
- 3: set $i = 0$
- 4: set $\mathbf{a}_r^i = \mathbf{a}_r^0$, $\mathbf{x}^i = \mathbf{x}^0$, $\dot{\mathbf{x}}^i = \dot{\mathbf{x}}^0$
- 5: for $i \leftarrow 0, N-1$ **do**
- 6: calculate the weighting coefficients $[\alpha_1, \alpha_2, \dots, \alpha_{s_1}]$, $[\beta_1, \beta_2, \dots, \beta_{s_2}]$ at \mathbf{a}_r^i and \mathbf{x}^i using the weighting functions (27), (24)

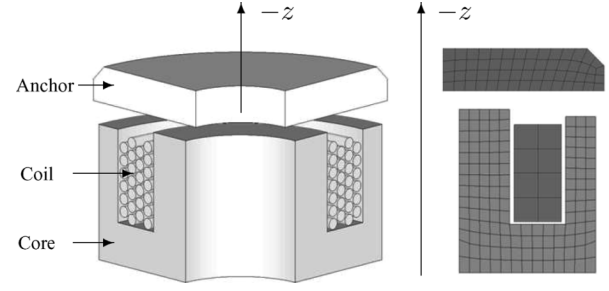


Fig. 3. A simple electromagnetic device consisting of: a magnetic core, a moving anchor, a coil, and a mechanical spring (not shown in the figure). The 3-D model (left) is shown for illustration purposes, whereas the spatially discretized 2-D model (right)—rotation symmetric around the z -axis—was used for the device simulation.

- 7: Simulate the reduced-order model (21) in the time span $[t^i, t^{i+1}]$ to find \mathbf{a}_r^{i+1} , $\mathbf{f}_{\text{mag}}^{i+1}$
 - 8: Simulate the mechanical equations (19) in the time span $[t^i, t^{i+1}]$ to find \mathbf{x}^{i+1} , $\dot{\mathbf{x}}^{i+1}$
 - 9: set $i = i + 1$, $\mathbf{a}_r^i = \mathbf{a}_r^{i+1}$, $\mathbf{x}^i = \mathbf{x}^{i+1}$, $\dot{\mathbf{x}}^i = \dot{\mathbf{x}}^{i+1}$
 - 10: **end for**
-

It is worth mentioning that the quadratic output equation in (22) keeps the overall approximation model of EM field (21), (22) nonlinear even after linearizing the nonlinear term in the differential equation (21). Therefore the POD method is chosen for reducing the order of the ensemble of models (22) due to its ability to reduce the order of nonlinear dynamic systems.

V. SIMULATION RESULTS

In this section, the proposed order reduction scheme is applied to generate a fast simulation model of a magnetic device with nonlinear magnetic materials (Fig. 3). The device consists of a coil, a ferromagnetic core, a moving anchor, and a mechanical spring between the anchor and the magnetic core. The device is modeled using a 2-D model and spatially discretized using the coupled BEM-FEM method. The spatial discretization of the magneto(quasi)static electromagnetic field equations resulted in a system of nonlinear differential algebraic equations DAEs of order $n = 837$. The algebraic part is removed by elimination to get a system of nonlinear ordinary differential equations (18) of order $n = 629$. The movement of the anchor is restricted to a one dimensional translation of its center of gravity along the z -axis and modeled using (19). The bumps at the end of both movement directions limit the anchors movement to the range $z \in [0, 400] \mu\text{m}$.

Three simulation runs of the full-order nonlinear model (18), (19) were performed using excitation signals of maximal amplitudes of 4, 8, and 15 A, respectively (Fig. 4). The simulation step size was chosen to be $\Delta t = 5 \mu\text{s}$, and the number of simulation steps per run is set to 300. The aforementioned settings of the simulation time steps have been fixed for all the simulation runs presented in this work including the simulation runs of the reduced-order model. The nonlinear term $\mathbf{K}(\mathbf{a})\mathbf{a}$ is linearized at all the simulation steps along the three simulation trajectories.

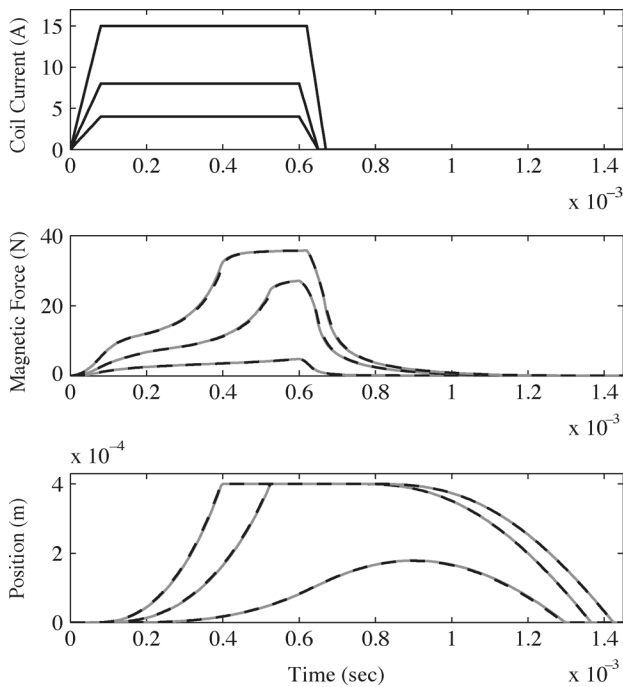


Fig. 4. Simulation results using training excitation signals: full-order nonlinear model $n = 837$ (continuous line) versus reduced-order model $n = 60$ (dashed line).

This resulted in $s_1 = 900$ linearized functions (20). The output matrix $\mathbf{R}(\mathbf{x})$ and the boundary matrix $\mathbf{K}^{\text{BEM}}(\mathbf{x})$ are extracted at $s_2 = 50$ uniformly distributed positions within the movement range $[0, 400] \mu\text{m}$. The solution vectors of the high-order nonlinear model (18) are assembled in a snapshots matrix, and the proper orthogonal decomposition is applied to extract the optimal orthonormal basis vectors. A total number of $k = 60$ orthonormal vectors were needed to achieve a good approximation of the snapshots matrix. The generated reduced-order electromagnetic field model (25), (26) of order $n = 60$ is weakly coupled to the mechanical equations (19) and simulated using the same excitation signals that were used to generate the training trajectories.

The simulation results in Fig. 4 show an excellent matching between the full-order and the reduced-order models considering both the output of the electromagnetic field model (*the magnetic force acting on the anchor*), and the output of the weakly coupled mechanical equation (*anchor's position*). For the purpose of validation, both models are simulated using two input signals of maximal amplitudes of 6 and 12 A, respectively. The simulation results in Fig. 5 show an excellent matching between both models, with the reduced-order model being approximately 50 times faster than the original model in all simulation runs as it is shown in Table I.

Further validation runs using excitation signals of maximal amplitudes of 30 and 50 A, respectively, have shown a degradation in the approximation accuracy of the reduced-order model. This behavior was expected, as the new input signals—that have much higher amplitudes than all of the training signals—drive the simulation trajectories to new regions of the state space of the original model (18). In those regions, the behavior of

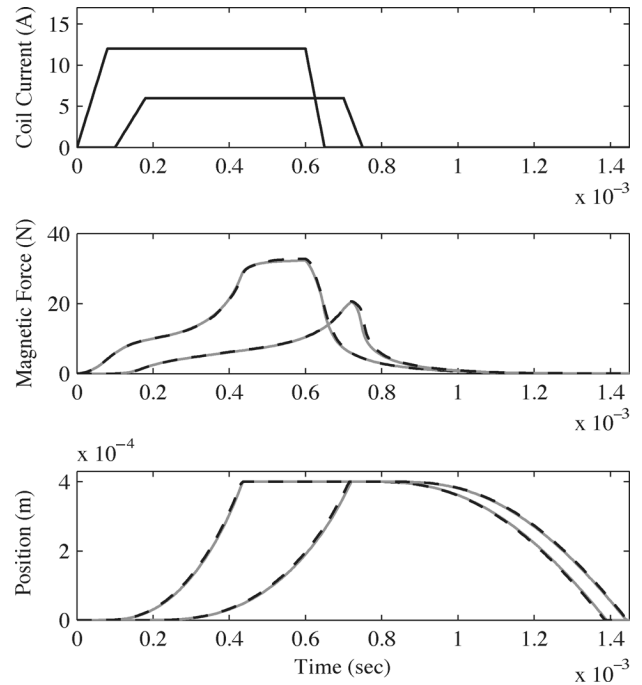


Fig. 5. Simulation results using validation excitation signals: full-order nonlinear model $n = 837$ (continuous line) versus reduced-order model $n = 60$ (dashed line).

TABLE I
SIMULATION TIME: FULL-ORDER NONLINEAR MODEL VERSUS
REDUCED-ORDER MODEL

Coil Current (Amperes)	Simulation Time (sec)	
	Full Order Nonlinear Model $n = 837$	Reduced Order Model $n = 60$
15	554	11.65
12	579	11.93
8	582	10.60
6	549	11.64
4	544	11.84

the nonlinear function $\mathbf{K}(\mathbf{a})\mathbf{a}$ is unknown to the model (25) and cannot be well approximated as a weighted sum of the existing s_1 linearized models in it. However, this degradation was alleviated by linearizing the nonlinear term $\mathbf{K}(\mathbf{a})\mathbf{a}$ at several points along the new simulation trajectories, and appending the new linearization points—after reducing their order—to the set $\{\mathbf{a}_{r1}, \dots, \mathbf{a}_{rs1}\}$ which is used by the weighting function (27). Additionally, the new linearized terms $\mathbf{L}_i, \mathbf{g}_i$ are appended to the ensemble of linearized models in (25) after reducing their order. This shows that the validity range of the proposed reduced-order models can be expanded successively when required, without the need to repeat the model generation procedure from the very beginning.

Finally, it has been noticed that the accuracy of the reduced-order model improves slightly when simulating it using smaller time steps ($\Delta t < 5 \mu\text{s}$). This can be traced back to the finer interpolation of the approximated terms in (25), (26). However, it is not trivial to make a general judgment regarding the maximal allowed size of the simulation step Δt . This is due to the fact that

all simulation models that are based on the weak electromechanical coupling approach—including the original full-order nonlinear model—suffer from the lack of accuracy if the size of simulation time step is not chosen adequately.

VI. CONCLUSION

In this work, we presented a new approach for generating fast simulation models of electromagnetic devices using model-order reduction techniques. The approach is based on approximating the high-dimensional spatially discretized models of electromagnetic field by reduced-order ones, that are able to reproduce the behavior of the original models and their variations under both components movement and materials nonlinearity. A major advantage of the proposed approach is in its ability to decouple the approximation of the model variations that are caused by components movement from the ones that are induced by the nonlinearity of magnetic materials, as this provides the possibility to control the approximation accuracy of both variation types independently. Moreover, the decoupled approximation of the position-dependent terms allows coupling the reduced-order EM field models weakly to any parametric mechanical system in order to simulate components movement. This makes the overall coupled electromagnetic-mechanical models parametric, and enables their use in the design optimization and robustness analysis of the modeled systems, which is expected to produce a remarkable speed up in the required time and computational resources in comparison to using the original models. This is currently being investigated in our ongoing research.

REFERENCES

- [1] A. C. Antoulas, *Approximation of Large Scale Dynamical Systems*. Philadelphia, PA: Society for Industrial and Applied Mathematics, 2006.
- [2] P. Astrid and S. Weiland, "On the construction of POD models from partial observations," in *Proc. 44th IEEE Conf. Decision and Control, and the Eur. Control Conf.*, Dec. 2005.
- [3] A. Bossavit, *Computational Electromagnetism*. New York: Academic, 1998.
- [4] B. Boualem and F. Piriou, "Numerical models for rotor cage induction machines using finite element method," *IEEE Trans. Magn.*, vol. 34, no. 5, pp. 3202–3205, Sep. 1998.
- [5] A. C. Cangellaris, M. Celik, S. Pasha, and L. Zhao, "Electromagnetic model order reduction for system level modeling," *IEEE Trans. Microw. Theory Tech.*, vol. 47, no. 6, pp. 840–850, Jun. 1999.
- [6] M. Clemens, M. Wilke, R. Schuhmann, and T. Weiland, "Subspace projection extrapolation scheme for transient field simulations," *IEEE Trans. Magn.*, vol. 40, no. 2, pp. 934–937, Mar. 2004.
- [7] M. Costabel and M. Dauge, "Singularities of electromagnetic fields in polyhedral domains," *Arch. Ration. Mech. Anal.*, vol. 151, no. 3, pp. 221–276, 2000.
- [8] R. S. Elliott, *Electromagnetics: History, Theory and Applications*, ser. IEEE/OUP Series on Electromagnetic Wave Theory. New York: Wiley-IEEE Press, 1999.
- [9] F. Henrotte, A. Nicolet, H. Hédia, A. Genon, and W. Legros, "Modeling of electromechanical relays taking into account movement and electric circuits," *IEEE Trans. Magn.*, vol. 30, no. 5, pp. 3236–3239, Sep. 1994.
- [10] S. Kurz, J. Fetzer, and G. Lehner, "Three dimensional transient BEM-FEM coupled analysis of electrodynamic levitation problems," *IEEE Trans. Magn.*, vol. 32, no. 3, pp. 1062–1065, May 1996.
- [11] V. Leconte, V. Mazauric, G. Meunier, and Y. Maréchal, "Remeshing procedures compared to FEM-BEM coupling to simulate the transients of electromechanical devices," in *Proc. CEFC*, 2000, p. 227.
- [12] Y. C. Liang, H. P. Lee, S. P. Lim, W. Z. Lin, K. H. Lee, and C. G. Wu, "Proper orthogonal decomposition and its applications, Part I: Theory," *J. Sound Vib.*, vol. 252, no. 3, pp. 527–544, May 2002.
- [13] S. Mijalkovic, "Truly nonlinear model-order reduction techniques," in *Proc. IEEE 7th Int. Conf. Thermal, Mechanical and Multiphysics Simulation and Experiments in Micro-Electronics and Micro-Systems (EuroSimE)*, 2006, pp. 1–5.
- [14] J. Philips, "A statistical perspective on nonlinear model reduction," in *Proc. IEEE Int. Workshop on Behavioral Modeling and Simulation (BMAS)*, 2003.
- [15] L. Qu and P. L. Chapman, "Extraction of low-order non-linear inductor models from a high-order physics-based representation," *IEEE Trans. Power Electron.*, vol. 21, no. 3, pp. 813–817, May 2006.
- [16] O. Rain, B. Auchmann, S. Kurz, V. Rischmuller, and S. Rjasanow, "Edge-based BE-FE coupling for electromagnetics," *IEEE Trans. Magn.*, vol. 24, no. 4, pp. 679–682, Apr. 2006.
- [17] M. Rewienski and J. White, "A trajectory piecewise-linear approach to model order reduction and fast simulation of nonlinear circuits and micromachined devices," *IEEE Trans. Comput.-Aided Des. Integr. Circuits Syst.*, vol. 22, no. 2, pp. 155–170, Feb. 2003.
- [18] V. Rischmuller, *Eine Parallelisierung der Kopplung der Methode der finiten Elemente und der Randelementmethode*, ser. 21. Berlin, Germany: VDI Verlag, 2005, no. 336.
- [19] V. Rischmuller, J. Fetzer, M. Haas, S. Kurz, and W. M. Rucker, "Computational efficient BEM-FEM coupled analysis of 3-D nonlinear eddy current problems using domain decomposition," in *Proc. 8th Int. IGTE Symp. Numerical Field Calculation*, 1998.
- [20] M. Simeoni, G. A. E. Vandenbosch, and I. E. Lager, "Model order reduction techniques for linear electromagnetic problems—An overview," in *Eur. Microwave Conf.*, 2005, vol. 2.
- [21] T. Wittig, I. Munteanu, R. Schuhmann, and T. Weiland, "Two-step Lanczos algorithm for model order reduction," *IEEE Trans. Magn.*, vol. 38, no. 2, pp. 673–676, Mar. 2002.
- [22] H. Wu and A. C. Cangellaris, "Model-order reduction of finite-element approximations of passive electromagnetic devices including lumped electrical-circuit models," *IEEE Trans. Microw. Theory Tech.*, vol. 52, no. 9, pp. 2305–2313, Sep. 2004.

Manuscript received December 20, 2007; revised February 29, 2008. Corresponding author: M. Nassar Albunni (e-mail: nassar.albunni@de.bosch.com).